Heliyon 9 (2023) e21549

Contents lists available at ScienceDirect

Heliyon

journal homepage: www.cell.com/heliyon

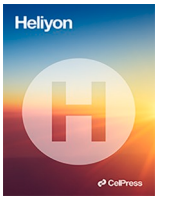

Tetramethylpyrazine promotes angiogenesis and nerve regeneration and nerve defect repair in rats with spinal cord injury

ZengTao Hao *, Chao Yin, XiaoLong Wang, ZhiQi Huo, GuoRong Zhang, Dong Jiang, Min An **

Department of Hand and Foot Microsurgery, Second Affiliated Hospital of Inner Mongolia Medical University, Hohhot City, 010000, China

A R T I C L E I N F O

Keywords:
Tetramethylpyrazine
miR-497-5p
EGFL7
Angiogenesis
Spinal cord injury
Nerve regeneration
Nerve defect repair

A B S T R A C T

Objective: This study evaluated the regulatory effect of Tetramethylpyrazine (TMP) on the spinal cord injury (SCI) rat model and clarified the neuroprotective mechanism of TMP on SCI.
Methods: An SCI rat model was generated and treated with TMP injections for two weeks. miR-497-5p and EGFL7 expression changes were evaluated, motor function recovery after SCI was assessed by BBB score test and footprint analysis, lesions of rat spinal cord were assessed by HE staining and TUNEL staining; angiogenesis was assessed by immunoblotting for CD31; inflammatory factor levels were detected by ELISA. EGFL7 was verified as a target of miR-497-5p by bioinformatics website analysis and luciferase reporter gene assay. H_2O_2-injured neurons were cultured *in vitro* to explore the effect of TMP.
Results: After SCI, miR-497-5p was upregulated while EGFL7 was downregulated in rats. TMP inhibited apoptosis and promoted angiogenesis, nerve regeneration, and repair of nerve defects by reducing miR-497-5p and increasing EGFL7 expression. miR-497-5p targeted EGFL7. In addition, TMP hindered neuronal inflammation and apoptosis induced by H_2O_2 *in vitro*.
Conclusion: TMP promotes angiogenesis by downregulating miR-497-5p to target EGFL7, and promotes nerve regeneration and repair of nerve defects in rats with SCI.

1. Introduction

Spinal cord injury (SCI) is a serious injury to the central nervous system that can result in abnormal or loss of motor, sensory, and autonomic function [1]. There are 11,000 new SCI cases in the United States each year, and more than 60,000 new cases in China each year [2]. When primary spinal cord injury occurs, acute disruption of the microvascular structure occurs immediately, leading to the breakdown of the blood-spinal barrier, endothelial cell death, and increased vascular permeability [3]. These comprehensive vascular injuries trigger a series of secondary pathological processes, including inflammation, and the formation of glial and fibrotic scars, which further prevent tissue regeneration and functional recovery [4,5]. As an important structure for a stable supply of nutrients and oxygen, microvessels play a crucial role in neurogenesis and maintenance of physiological functions [6]. Angiogenesis refers to the generation of newly formed microvessels from the germination of original blood vessels or proliferation in the injury core [7].

* Corresponding author. Department of hand and foot microsurgery, Second Affiliated Hospital of Inner Mongolia Medical University, No. 59, Horqin Road, Saihan District, Hohhot City, 010000, China.
** Corresponding author. Department of Anesthesiology, Second Affiliated Hospital of Inner Mongolia Medical University, No. 59, Horqin Road, Saihan District, Hohhot City, 010000, China.
E-mail addresses: haozengtaomd2008@hotmail.com (Z. Hao), anmin5@163.com (M. An).

https://doi.org/10.1016/j.heliyon.2023.e21549
Received 5 January 2023; Received in revised form 25 August 2023; Accepted 23 October 2023
Available online 27 October 2023

Therefore, targeting angiogenesis early in SCI can reduce cell loss and neurological deficits. Intrathecal anti-NoGo-A antibodies in the treatment of SCI can improve vascular germination and repair and reduce neurological deficits [8,9]. This evidence confirms that angiogenesis plays a key role in nerve repair after SCI. Therefore, finding ways to enhance nerve regeneration and angiogenesis could aid recovery from SCI.

Tetramethylpyrazine (TMP), the main bioactive component of Ligusticum chuanxiong, exerts anti-inflammatory, antioxidant, neuroprotective, and axonal growth-promoting effects [10]. In addition, TMP can protect various cells by inhibiting the cascade of oxidative stress and apoptosis [11]. Due to these properties, TMP is of therapeutic potential in a variety of diseases, including SCI [12,13]. For example, TMP attenuates SCI-induced nerve injury by inhibiting vascular endothelial cell apoptosis and promoting angiogenesis [14]. TMP promotes the recovery of SCI through the Akt/Nrf2/HO-1 pathway [15]. However, the molecular mechanism of TMP in SCI has not been fully elucidated.

MicroRNAs (miRNAs) are a class of short non-coding RNAs that either silence translation or interfere with the expression of target mRNAs [16]. miRNAs are involved in the physiological and pathological processes of various diseases, such as cancer [17], nerve injury diseases [18], and cardiovascular diseases [19]. miR-497-5p is one of the members of the miR-15/107 family [20–22], and its expression profile in vascular diseases has been extensively studied. miR-497-5p is involved in melanoma [23], gastric cancer [24], and esophageal squamous cell carcinoma [25]. Besides, miR-497-5p regulates inflammation-related signaling pathways in hepatocellular carcinoma [26]. A previous study shows that miR-497-5p is upregulated in Parkinson's disease, and it could modulate neuronal apoptosis and autophagy [27]. In addition, miR-497-5p has also been shown to be involved in angiogenesis [28]. However, the role of miR-497-5p in SCI is unclear.

Epidermal growth factor-like domain-containing protein 7 (EGFL7), a member of the epidermal growth factor-like protein family, is a potent angiogenic factor expressed in many cell types. EGFL7 plays a vital role in controlling angiogenesis during embryogenesis, organogenesis, and maintenance of skeletal homeostasis [29]. Several studies have shown that EGFL7 can promote angiogenesis [30,31]. In addition, miR-497-5p was found to regulate EGFL7 expression.

This study aimed to investigate the effect of TMP on angiogenesis and nerve regeneration in SCI and its underlying mechanisms. *In vivo* and *in vitro* experiments revealed that TMP mediates miR-497-5p/EGFL7 axis to promote SCI angiogenesis, nerve regeneration, and nerve defect repair, providing a new direction for SCI treatment.

2. Materials and methods

2.1. SCI animal model

This study was approved by the Ethics Committee of Second Affiliated Hospital of Inner Mongolia Medical University (Ethics approval number: NM20170611DC). Sprague-Dawley rats (Animal Center of the Chinese Academy of Sciences, Shanghai, China) were fed in a specific pathogen-free environment for at least 48 h and treated with SCI referring to the modified Allen method [32]. Briefly, a laminectomy was performed on the T10 vertebrate with steel clips inserted under the transverse process. Contusions of 200 kdyn were performed using an IH spinal cord impactor (Precision Systems and Instrumentation, Lexington, KY). Sham operation rats were treated with laminectomy only.

2.2. Lentiviral treatment

After SCI, the injured spinal segment was treated with TMP (200 mg/kg/day) for two weeks. Meanwhile, SCI rats were intrathecally injected with antagomir NC (5′-CAGUACUUUUGUGUAGUACAA-3′), miR-497-5p antagomir (5′-ACAAACCACAGUGUGCUGCUG-3′), agomir NC (5′-UUCUCCGAACGUGUCACGUTT-3′), miR-497-5p agomir (5′-CAGCAGCACACUGUGGUUUGUAAACCACAGUGUGCUGCUGUU-3′), sh-NC (5′-UUCUCCGAACGUGUCACGUTT-3′), sh-EGFL7 (5′-AGCAGATTTCCTTCCTGGA-3′), oe-NC (5′-GTTCTCCGAACGTGTCACGT-3′), oe-EGFL7 (5′-GCTCTAGACCTGCAAGAAAGACTCGTGA-3′), miR-497-5p antagomir + sh-NC and miR-497-5p antagomir + sh-EGFL7, respectively. The lentiviral vectors used were constructed by Genepharma (Shanghai, China).

Table 1
Primer sequences used in PCR.

Genes	Sequences (5′– 3′)
miR-497-5p	F: CAGCAGCACACUGUGGUUUGUA
	R: CTCTACAGCTATATTGCCAGCCAC
EGFL7	F: GGGATGGCAGGGAGATACTTG
	R: CTGGCGTGGGACTTGGTG
U6	F: CTCGCTTCGGCAGCACA
	R: AACGCTTCACGAATTTGCGT
GAPDH	F: CGGAGTCAACGGATTTGGTCGTAT
	R: AGCCTTCTCCATGGTGGTGAAGAC

Note: F, forward; R, reverse; miR-497-5p, microRNA-497-5p; EGFL7, Epidermal growth factor-like domain 7; GAPDH, glyceraldehyde-3-phosphate dehydrogenase.

3. Detection of RNA expression

Total RNA was extracted from tissues or cells using Trizol reagent (Invitrogen, USA) and reverse-transcribed using SuperScript Reverse Transcription Kit (Invitrogen). On an ABI PRISM7900 Sequence Detection System (Applied Biosystems, USA), PCR was implemented with SYBR Green Master Mix (Applied Biosystems, USA). GAPDH and U6 were internal controls, and the relative expression levels were analyzed by the $2^{-\Delta\Delta Ct}$ method. The primers (Table 1) were synthesized by Sangon (Shanghai, China).

3.1. Western blot

Proteins were extracted using RIPA lysis buffer and quantified by a BCA protein assay kit (Beyotime, China). After being separated by 12 % SDS-PAGE, the samples were loaded onto polyvinylidene fluoride membranes (Bio-Rad, USA) which were then counteracted with primary antibodies EGFL7 (19291-1-AP, 1:500, Proteintech), CD31 (ab28364, 1:500, Abcam), and GAPDH (2118, 1:1000, CST) and co-incubated with the secondary antibody (ab6734, 1:3000, Abcam). Protein bands were visualized using chemiluminescent reagents (WBKLS0100, Millipore, USA). GAPDH was used as an internal reference, and Image J (V1.8.0, National Institutes of Health, USA) was used to analyze the levels of target proteins.

3.2. Basso, Beattie, and Bresnahan (BBB) score

Before SCI and 1, 3, 7, 14, and 21 days after SCI, respectively, the motor behavior of rats was assessed in the open field based on BBB score [33]. The preoperative BBB score of the rats was 21 points.

3.3. Footprint analysis

Rats run down a paper-covered hallway after their front and back PAWS are painted with different colors of non-toxic paint. Stride length and width were measured and analyzed while the rats ran at a constant speed. Each rat was assessed by two independent examiners who did not know about treatment options [34].

3.4. HE staining

After the BBB score, the rats were anesthetized with 3 % pentobarbital sodium and immediately intracardially perfused. Then, the spinal cord was exposed and approximately 2 cm of spinal cord tissue around the lesion site was excised and fixed in 4 % paraformaldehyde buffer to prepare paraffin slices with 5 μm thickness. Sections were dewaxed and hydrated, stained with hematoxylin for 5 min and 0.5 % eosin for 2 min. Then the sections were dehydrated with alcohol, cleared with xylene, and sealed with neutral resin. Finally, the spinal cord lesions of rats were observed under a microscope (Olympus) [35].

3.5. TUNEL staining

Paraffin slices with 5 μm thickness were dewaxed and hydrated with gradient alcohols for determining apoptosis using the TUNEL fluorescence FITC kit (Roche, USA). After TUNEL staining, DAPI staining (Sigma-Aldrich) was performed followed by fluorescence observation under a laser scanning confocal microscope (FV1000, Olympus, Japan) [36].

4. ELISA

Blood samples were centrifuged at 3000 g to obtain plasma. The concentrations of TNF-α, TGF-β, and IL-1β in the samples were determined using ELISA kits (R&D Systems, Inc., MN, USA).

4.1. H_2O_2-induced injury of primary neurons

Primary neurons were obtained from 4-day-old neonatal SD rats. Rat spinal cords were immersed in a D-Hank medium and centrifuged to collect the pellet. The pellet was treated with detachment with 0.25 % trypsin, which was stopped by 10 % FBS-DMEM. The neurons were incubated with Cytarabine (final concentration 3 mol/L) for 3 d and exposed to H_2O_2 [37]. DMSO-dissolved TMP (95162, Sigma) was administrated to H_2O_2-injured neurons at different concentrations (50 μg/ml; 100 μg/ml; 150 μg/ml) [38].

4.2. Flow cytometry

Apoptotic cells were detected by AnnexinVFITC/PI double staining according to the procedures [39]. In brief, the neurons were centrifuged at 2000 rpm for 5 min, washed twice with cold PBS, and suspended with 400 μL 1 × binding buffer. At 4 °C, the cell suspension was then added with 5 μL AnnexinV-FITC and incubated in dark for 15 min and 10 μL PI in dark for 5 min. Finally, the apoptosis rate was measured on a flow cytometer (BD FACS Calibur, BD, USA).

4.3. Targeting relation analysis

HEK293T cells (ATCC) were placed in 10 % FBS-DMEM supplemented with 1 mM glutamine, 100 units/ml penicillin, and 100 mg/ml streptomycin. According to the manufacturer's instructions, the luciferase reporter gene test was performed using the dual

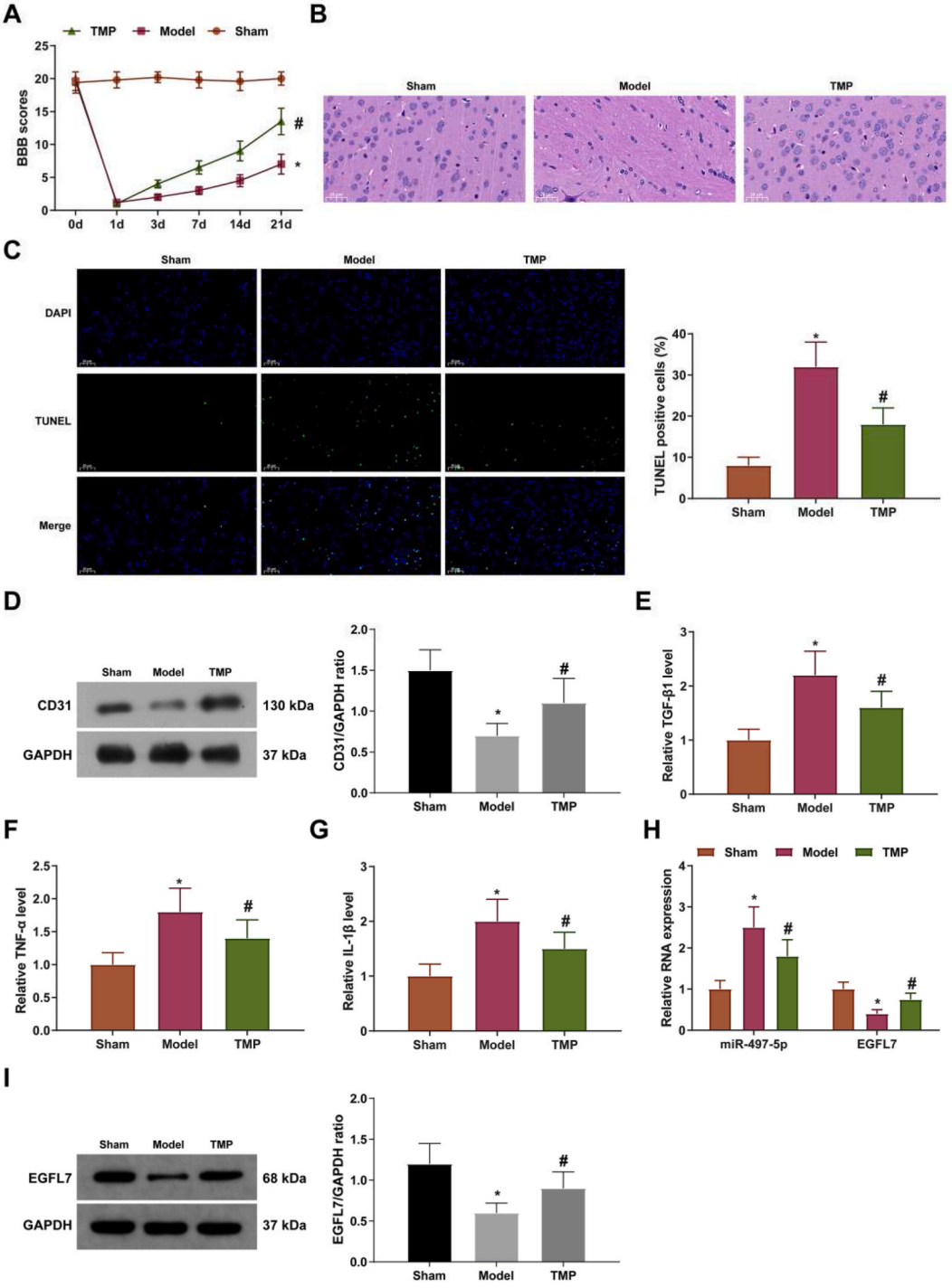

Fig. 1. TMP promotes angiogenesis, nerve regeneration and nerve defect repair in rats with SCI.
A: BBB score to test the motor behavior of rats; B–C: HE staining and TUNEL staining to assess the lesions of rat spinal cord; D: Western blot to detect CD31 expression to assess angiogenesis; E–G: ELISA to detect inflammatory factors; H–I: RT-qPCR or Western blot to detect miR-497-5p and EGFL7 expression; the values are expressed by the mean standard deviation. *$P < 0.05$ vs. Sham; #$P < 0.05$ vs. Model.

luciferase test kit (D0010, Solarbio, Beijing, China) [40]. In short, a reporter vector containing EGFL7 3 ′UTR and a mutant vector binding to miR-497-5p with mutant sites were constructed: pGL3-EGFL7-WT and pGL3-EGFL7-MUT. The vectors were co-transfected with miR-497-5p mimic or mimic NC into HEK293T cells. After 48 h, the cells were collected after lysis and tested for luciferase activity by a photometer. Renilla luciferase activity was used as the internal reference. The ratio of firefly luciferase activity to renilla luciferase activity is considered to be relative luciferase activity.

4.4. Statistical analysis

All data were analyzed using SPSS 17.0 (SPSS, IL, USA). To compare BBB scores, repeated measures analysis of variance (ANOVA) was performed followed by Bonferroni post hoc correction. One-way ANOVA with Tukey's post hoc test was utilized for comparing multiple sets of data. All data were presented as mean ± standard deviation (SD), and the significance cutoff was set at $P < 0.05$.

5. Results

5.1. TMP promotes angiogenesis, nerve regeneration and nerve defect repair in rats with SCI

Before SCI and 1, 3, 7, 14, 21 days after SCI, respectively, we evaluated the motor function of rats using a 21-point BBB score and discovered that Sham operation rats walked normally, and SCI rats had obvious walking deficits, while TMP treatment could improve walking deficits in SCI rats (Fig. 1A). In addition, the footprint analysis was used to evaluate the recovery of motor function in SCI rats, and the results showed that the length and width of SCI rats' stride decreased, and motor function was poor. However, after TMP treatment, the length and width of SCI rats' stride increased, and motor function was significantly improved (Supplementary Fig. 1A, Supplementary Fig. 2). The lesions of the rat spinal cord were evaluated by HE staining and TUNEL staining. No obvious apoptosis and necrosis was found in the spinal cord tissue of the sham operation rats; SCI rats showed neuronal atrophy and apoptosis, while SCI rats receiving TMP treatment presented improvements of pathological conditions (Fig. 1B and C). Angiogenesis was assessed by Western blot detection of CD31 expression, presenting that CD31 expression was decreased in SCI rats, while its expression trend could be recovered when TMP was administrated (Fig. 1D). ELISA detection suggested that SCI induced serum levels of inflammatory factors (TGF-β1, TNF-α and IL-1β) in rats, but this pro-inflammatory influence could be attenuated by TMP (Fig. 1E–G). In addition, we also

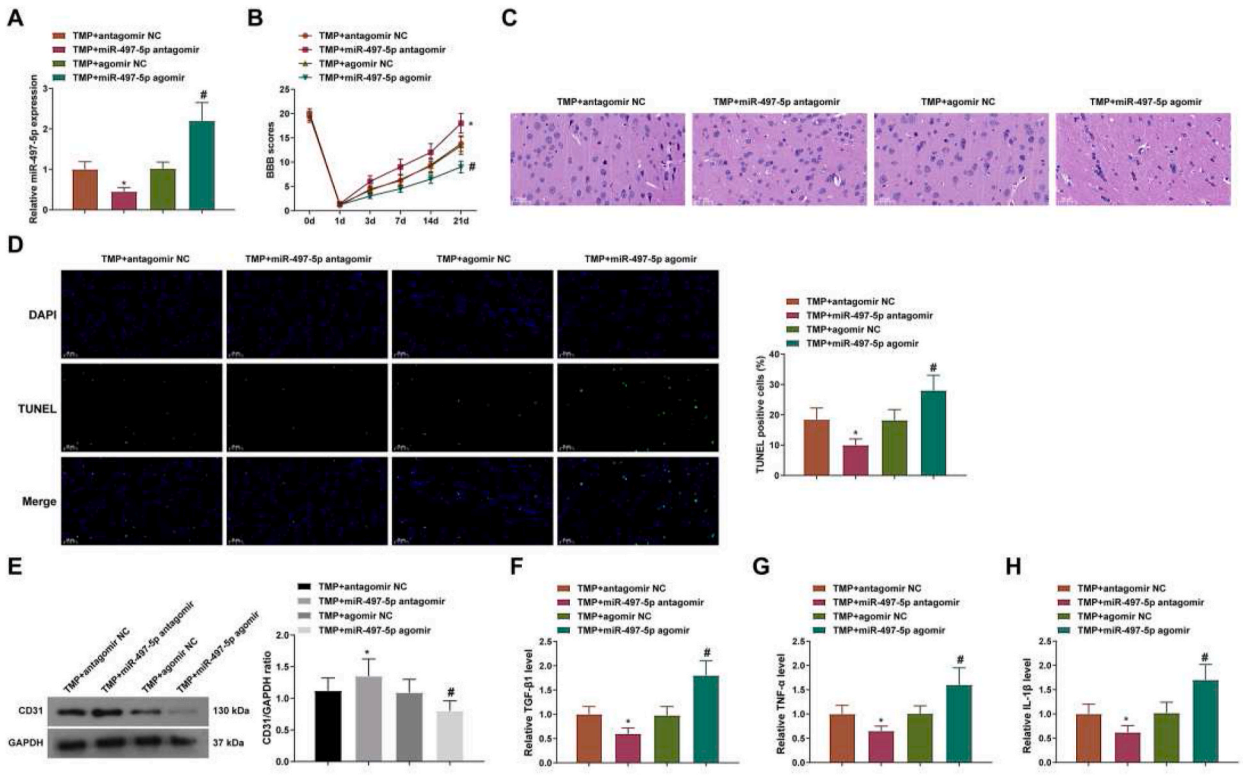

Fig. 2. Depleting miR-497-5p augments TMP-induced protection against SCI.
A: RT-qPCR to detect miR-497-5p expression; B: BBB score to test the motor behavior of rats; *C*–D: HE staining and TUNEL staining to assess the lesions of the rat spinal cord; E: Western blot to detect CD31 expression to assess angiogenesis; F–H: ELISA detects the levels of inflammatory factors; the values are expressed by the mean standard deviation. *$P < 0.05$ vs. TMP + antagomir NC; #$P < 0.05$ vs. TMP + agomir NC.

found miR-497-5p upregulation and EGFL7 downregulation in SCI rats, and TMP could inhibit miR-497-5p and promote EGFL7 expression levels (Fig. 1H and I).

5.2. Depleting miR-497-5p augments TMP-induced protection against SCI

When exploring the effect of miR-497-5p on SCI rats, rats were intrathecally injected with antagomir NC, miR-497-5p antagomir, agomir NC and miR-497-5p agomir lentivirus at the same time as TMP treatment. RT-qPCR verified that the injection was successful (Fig. 2A). BBB score results showed that down-regulation of miR-497-5p could further improve walking defects in SCI rats, while up-regulation of miR-497-5p could reverse the therapeutic effect of TMP (Fig. 2B). Footprint analysis showed that down-regulation of miR-497-5p could further improve motor function in SCI rats, while up-regulation of miR-497-5p could reverse the improvement of TMP (Supplementary Fig. 1B, Supplementary Fig. 2). HE staining and TUNEL staining showed that the pathological conditions of the spinal cord tissue of rats were further improved after downregulation of miR-497-5p, while the effect of up-regulation of miR-497-5p was opposite (Fig. 2C and D). Western blot results showed that CD31 expression was significantly increased after down-regulation of miR-497-5p, while up-regulation of miR-497-5p weakened the therapeutic effect of TMP (Fig. 2E). ELISA results showed that down-regulation of miR-497-5p could further reduce the contents of TGF-β1, TNF-α, and IL-1β in serum of SCI rats, while up-regulation of miR-497-5p had the opposite effect (Fig. 2F–H). As detected, depleting miR-497-5p augments TMP-induced protection against SCI.

5.3. miR-497-5p represses EGFL7 expression

The bioinformatics website predicted the targeted binding sites for miR-497-5p and EGFL7 (Fig. 3A). A dual-luciferase reporter gene assay was then performed to obtain the outcome that miR-497-5p mimic reduced the luciferase activity of pGL3-EGFL7-WT (Fig. 3B). EGFL7 expression was reduced when miR-497-5p was upregulated, and vice versa (Fig. 3C and D). In conclusion, miR-497-5p downregulates EGFL7.

5.4. EGFL7 upregulation promotes TMP-mediated protection in SCI rats

For understanding the action of EGFL7 on SCI rats, at the same time as TMP treatment, rats were intrathecally injected with oe-NC, oe-EGFL7, sh-NC and sh-EGFL7 lentiviruses, respectively, thus altering EGFL7 expression (Fig. 4A). BBB score results reported that up-regulation of EGFL7 could further improve walking defects in SCI rats, while down-regulation of EGFL7 could reverse the therapeutic effect of TMP (Fig. 4B). The results of footprint analysis revealed that up-regulation of EGFL7 further improved motor function in SCI rats, while down-regulation of EGFL7 reversed TMP's improvement effects on SCI rats (Supplementary Fig. 1C, Supplementary Fig. 2). HE staining and TUNEL staining observed that the pathological conditions of the spinal cord of rats were further improved after EGFL7 up-regulation, while the effect of EGFL7 down-regulation was opposite (Fig. 4C and D). Western blot noted that CD31 expression was

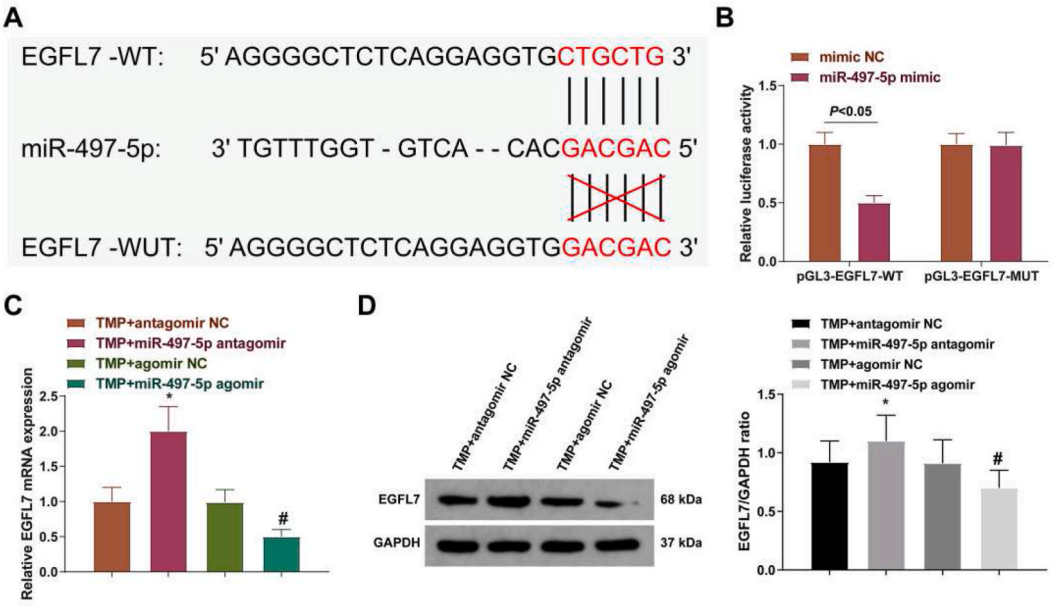

Fig. 3. MiR-497-5p inhibits EGFL7 expression.
A: Bioinformatics website to predict that miR-497-5p and EGFL7 have targeted binding sites; B: Dual-luciferase reporter gene detection to confirm the targeting relationship between miR-497-5p and EGFL7; C–D: RT-qPCR and Western blot to detect EGFL7 expression; the values were expressed by the mean standard deviation. *$P < 0.05$ vs. TMP + antagomir NC; #$P < 0.05$ vs. TMP + agomir NC.

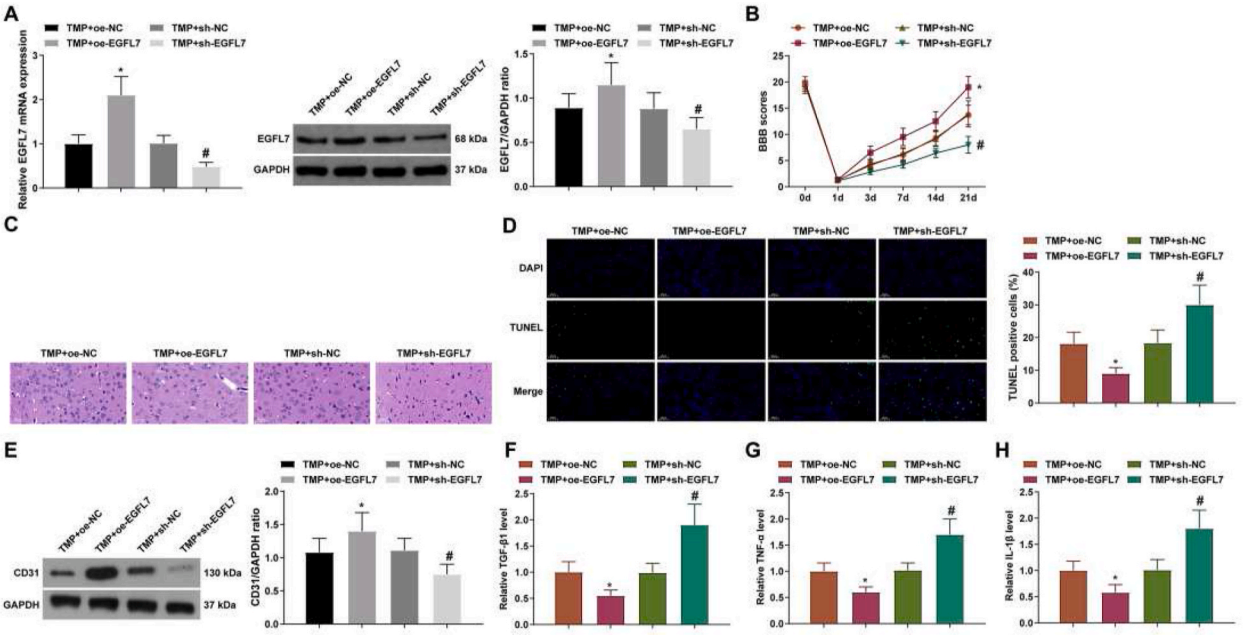

Fig. 4. EGFL7 upregulation promotes TMP-mediated protection on SCI rats.
A: RT-qPCR or Western blot to detect EGFL7 expression; B: BBB score to test the motor behavior of rats; *C*–D: HE staining and TUNEL staining to assess the lesions of the rat spinal cord; E: Western blot to detect CD31 expression to assess angiogenesis; F–H: ELISA detects the levels of inflammatory factors; the values are expressed by the mean standard deviation. $^{*}P < 0.05$ vs. TMP + oe-NC; $\#P < 0.05$ vs. TMP + sh-NC.

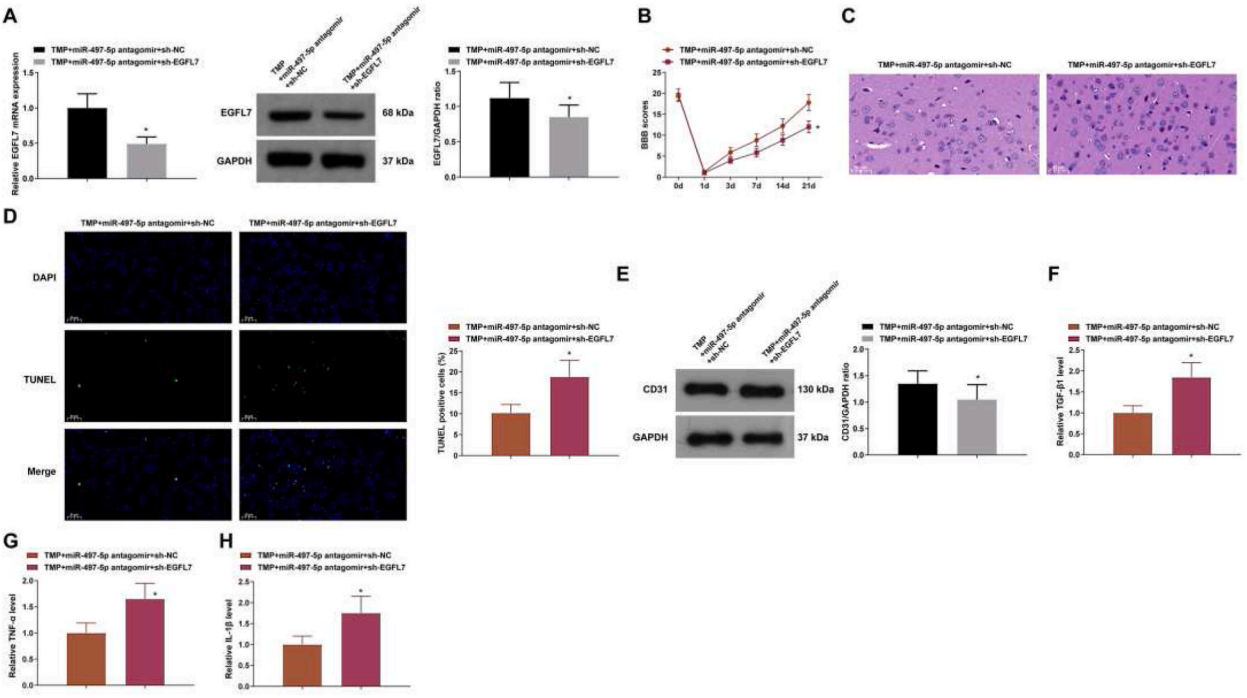

Fig. 5. EGFL7 inhibition resists miR-497-5p silencing-induced protection against SCI.
A: RT-qPCR or Western blot to detect EGFL7 expression; B: BBB score to test the motor behavior of rats; *C*–D: HE staining and TUNEL staining to assess the lesions of the rat spinal cord; E: Western blot to detect CD31 expression to assess angiogenesis; F–H: ELISA detects the levels of inflammatory factors; the values are expressed by the mean standard deviation. $^{*}P < 0.05$ vs. TMP + miR-497-5p antagomir + sh-NC.

significantly increased after EGFL7 was up-regulated, while the therapeutic effect of TMP was weakened when EGFL7 was down-regulated (Fig. 4E). ELISA results suggested that upregulation of EGFL7 could further reduce the contents of TGF-β1, TNF-α, and IL-1β in serum of SCI rats, while downregulation of EGFL7 had the opposite effect (Fig. 4F–H). In summary, EGFL7 upregulation promotes TMP-mediated protection in SCI rats.

5.4.1. EGFL7 inhibition resists miR-497-5p silencing-induced protection against SCI

To verify that TMP mediates miR-497-5p/EGFL7 axis to protect against SCI, rats were intrathecally injected with miR-497-5p antagomir + sh-NC or miR-497-5p antagomir + sh-EGFL7 lentivirus at the same time as TMP treatment. As the results suggested, sh-EGFL7-induced downregulation of EGFL7 prevented the therapeutic efficacy of miR-497-5p antagomir in SCI rats (Fig. 5A–H; Supplementary Fig. 1D, Supplementary Fig. 2).

5.5. TMP has a protective effect on H_2O_2-injured neurons

We further verified the protective effects of TMP on SCI through *in vitro* experiments. H_2O_2-treated neurons were treated with different concentrations of TMP (50 μg/ml; 100 μg/ml; 150 μg/ml), and flow cytometry was used to detect neuronal apoptosis. It was found that H_2O_2 significantly induced neuronal apoptosis, while TMP reduced neuronal apoptosis in a dose-dependent manner (Fig. 6A). In addition, the levels of inflammatory cytokines (TGF-β1, TNF-α, and IL-1β) were also significantly reduced after TMP treatment in a dose-dependent manner (Fig. 6B–D). These results are also consistent with previous *in vivo* data.

6. Discussion

SCI is a highly disabling disease with a series of destructive behaviors following the initial injury, including neurological damage, inflammation, and oxidative stress [41]. Although treatments or restorative treatments have been developed to slow or stop the progression of SCI, no method has yet been able to fully heal SCI. TMP has been shown to exert neuroprotective effects on SCI [14]. Therefore, exploring the potential mechanism of TMP in SCI is helpful to understand the pathogenesis of SCI and develop effective SCI treatment strategies. Our study functionally revealed that TMP can promote angiogenesis, nerve regeneration, and nerve defect repair in SCI rats as well as inhibit apoptosis and inflammation of H_2O_2-injured neurons. Mechanistically, SCI promoted EGFL7 expression by downregulating miR-497-5p.

For a long time, TMP has been a clinical option for cardiovascular diseases [42]. Recently, more and more studies have shown that TMP has a neuroprotective function. Zhang Li et al. [43] have stated that TMP can promote the proliferation and differentiation of neural stem cells and inhibit oxidative stress-induced apoptosis. Hu Jie et al. have reported that TMP has a protective effect on SCI rats, and TMP treatment reduces neuronal loss and promotes angiogenesis and neurological recovery after SCI [44]. Multiple studies have shown that TMP promotes neurological recovery after SCI by regulating multiple pathways [45,46] and TMP could suppress inflammatory cell activation and pro-inflammatory cytokine production to ameliorate SCI [47]. Our study analysis once again confirmed the protective effect of TMP on SCI: TMP treatment promoted angiogenesis, nerve regeneration, and repair of nerve defects in SCI rats, and inhibited neuronal apoptosis and the production of pro-inflammatory cytokines. As stated previously, TMP limits neuronal apoptosis in SCI by downregulating miR-214-3p [48]. Our paper demonstrated that TMP administration inhibited miR-497-5p expression, a finding suggesting that the role of TMP in SCI may be related to miR-497-5p.

In past studies, miR-497-5p has been indicated in a variety of human diseases, including cancer [49], diabetes [50], and neurological diseases [27]. This study initially discovered that miR-497-5p was upregulated in SCI rats and depleting miR-497-5p based on TMP treatment could further attenuate SCI-induced damages in rats and H2O2-induced apoptosis and inflammation in neurons while restoring miR-497-5p partially limited the treatment effect of TMP. Furthermore, we recognized that miR-497-5p was negatively correlated with EGFL7 expression in SCI rats and TMP administration inhibited miR-497-5p and promoted EGFL7 levels.

EGFL7 is a conserved secreted angiogenic factor that is involved significantly in angiogenesis [51]. It is mainly expressed during vascular development and promotes angiogenesis by controlling various endothelial molecular mechanisms [29]. Our experimental analysis found that EGFL7 expression was decreased in SCI rats, and restoring EGFL7 could enhance the therapeutic effect of TMP on SCI, while silencing EGFL7 reversed the therapeutic effects of TMP or inhibition of miR-497-5p on SCI.

However, there are some limitations in this study. Firstly, the number of experimental animals used in this study is small, so there may be some errors in this study. Secondly, TMP can regulate a variety of miRNAs, but only miR-497-5p was selected in this study. Third, there are many target genes of miR-497-5p, but only EGFL7 was selected for exploration in this study. Finally, the downstream regulatory mechanisms of EGFL7 were not further explored. It is hoped that in the future we can further explore more possible regulatory mechanisms of TMP's neuroprotective effect in SCI rats.

7. Conclusion

The study results presented that TMP promotes angiogenesis, nerve regeneration, and repair of nerve defects after SCI by downregulating miR-497-5p to modulate EGFL7 expression. This result not only contributes to the understanding of the mechanism of SCI but also provides a new reference for the development of new SCI treatments.

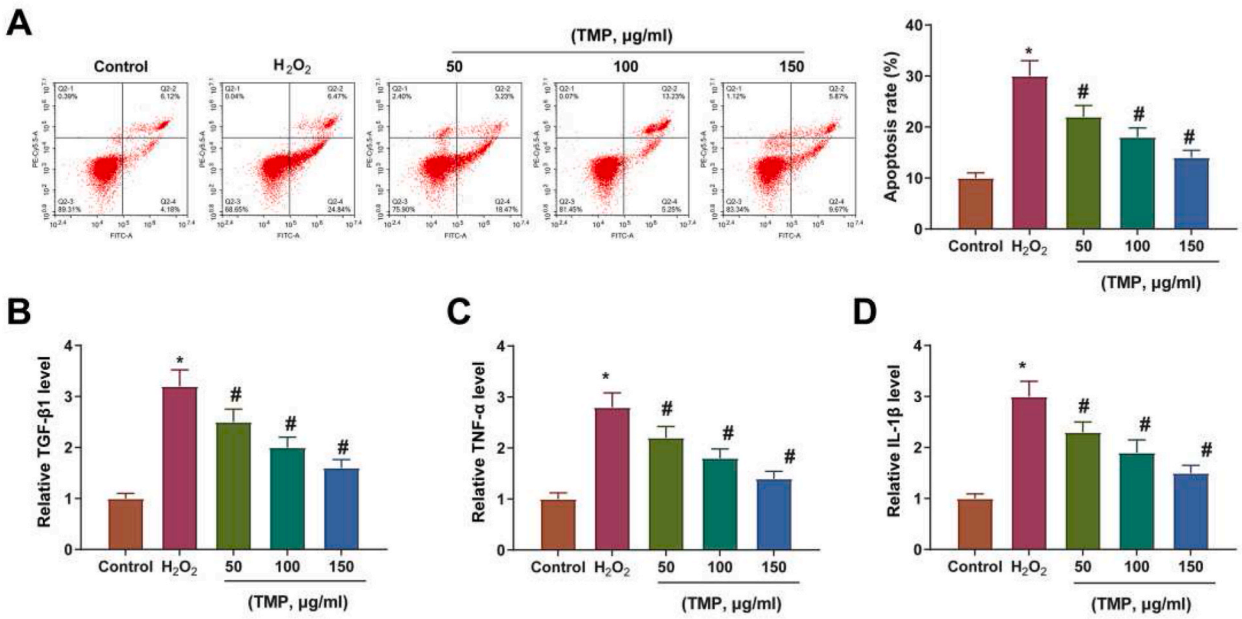

Fig. 6. TMP has a protective effect on H_2O_2-injured neurons.
A: Flow cytometry to detect cell apoptosis; B–D: ELISA to detect the levels of inflammatory factors; the values are represented by the mean standard deviation. $*P < 0.05$ vs. Control; $\#P < 0.05$ vs. H_2O_2.

Author contribution statement

ZengTao Hao: Conceived and designed the experiments; Performed the experiments; Wrote the paper. Chao Yin: XiaoLong Wang: Analyzed and interpreted the data. ZhiQi Huo: Contributed reagents, materials, analysis tools or data. GuoRong Zhang: Dong Jiang: Performed the experiments. Min An: Conceived and designed the experiments; Wrote the paper.

Data availability statement

Data will be made available on request.

Funding

Not applicable.

Ethical approval

All animal experiments were complied with the ARRIVE guidelines and performed in accordance with the National Institutes of Health Guide for the Care and Use of Laboratory Animals. The experiments were approved by the Institutional Animal Care and Use Committee of Second Affiliated Hospital of Inner Mongolia Medical University (Ethics approval number: NM20170611DC).

Declaration of competing interest

The authors declare that they have no known competing financial interests or personal relationships that could have appeared to influence the work reported in this paper.

Acknowledgments

Not applicable.

Appendix A. Supplementary data

Supplementary data to this article can be found online at https://doi.org/10.1016/j.heliyon.2023.e21549.

References

[1] X.D. Guo, X.G. He, F.G. Yang, M.Q. Liu, Y.D. Wang, D.X. Zhu, G.Z. Zhang, Z.J. Ma, X.W. Kang, Research progress on the regulatory role of microRNAs in spinal cord injury, Regenerative medicine 16 (2021) 465–476, https://doi.org/10.2217/rme-2020-0125.

[2] L. Yang, D. Ge, X. Chen, C. Jiang, S. Zheng, miRNA-544a regulates the inflammation of spinal cord injury by inhibiting the expression of NEUROD4, Cell. Physiol. Biochem. : international journal of experimental cellular physiology, biochemistry, and pharmacology 51 (2018) 1921–1931, https://doi.org/10.1159/000495717.

[3] S.A. Figley, R. Khosravi, J.M. Legasto, Y.F. Tseng, M.G. Fehlings, Characterization of vascular disruption and blood-spinal cord barrier permeability following traumatic spinal cord injury, J. Neurotrauma 31 (2014) 541–552, https://doi.org/10.1089/neu.2013.3034.

[4] C.S. Ahuja, J.R. Wilson, S. Nori, M.R.N. Kotter, C. Druschel, A. Curt, M.G. Fehlings, Traumatic spinal cord injury, Nat. Rev. Dis. Prim. 3 (2017), 17018, https://doi.org/10.1038/nrdp.2017.18.

[5] A.P. Tran, P.M. Warren, J. Silver, The biology of regeneration failure and success after spinal cord injury, Physiol. Rev. 98 (2018) 881–917, https://doi.org/10.1152/physrev.00017.2017.

[6] P. Sapieha, Eyeing central neurons in vascular growth and reparative angiogenesis, Blood 120 (2012) 2182–2194, https://doi.org/10.1182/blood-2012-04-396846.

[7] M.T. Ng, A.T. Stammers, B.K. Kwon, Vascular disruption and the role of angiogenic proteins after spinal cord injury, Translational stroke research 2 (2011) 474–491, https://doi.org/10.1007/s12975-011-0109-x.

[8] B. Zörner, M.E. Schwab, Anti-Nogo on the go: from animal models to a clinical trial, Ann. N. Y. Acad. Sci. 1198 (Suppl 1) (2010) E22–E34, https://doi.org/10.1111/j.1749-6632.2010.05566.x.

[9] R. Rust, L. Grönnert, C. Gantner, A. Enzler, G. Mulders, R.Z. Weber, A. Siewert, Y.D.P. Limasale, A. Meinhardt, M.A. Maurer, et al., Nogo-A targeted therapy promotes vascular repair and functional recovery following stroke, Proc. Natl. Acad. Sci. U.S.A. 116 (2019) 14270–14279, https://doi.org/10.1073/pnas.1905309116.

[10] L. Xu, J. Shen, S. Dai, L. Sun, X. Chen, Tetramethylpyrazine attenuated sevoflurane-induced neurotoxicity by enhancing autophagy through GPR50/CREB pathway in SH-SY5Y cells, Am. J. Chin. Med. 48 (2020) 945–966, https://doi.org/10.1142/s0192415x20500457.

[11] Q. Zhou, S. Chen, H. Li, B. Yang, T. Chen, T. Hu, D. Yin, H. He, M. He, Tetramethylpyrazine alleviates iron overload damage in vascular endothelium via upregulating DDAHII expression, Toxicol. Vitro : an international journal published in association with BIBRA 65 (2020), 104817, https://doi.org/10.1016/j.tiv.2020.104817.

[12] J. Li, J. Wei, Y. Wan, X. Du, X. Bai, C. Li, Y. Lin, Z. Liu, M. Zhou, Z. Zhong, TAT-modified tetramethylpyrazine-loaded nanoparticles for targeted treatment of spinal cord injury, J. Contr. Release : official journal of the Controlled Release Society 335 (2021) 103–116, https://doi.org/10.1016/j.jconrel.2021.05.016.

[13] W. Sun, A. Li, Z. Wang, X. Sun, M. Dong, F. Qi, L. Wang, Y. Zhang, P. Du, Tetramethylpyrazine alleviates acute kidney injury by inhibiting NLRP3/HIF-1α and apoptosis, Mol. Med. Rep. 22 (2020) 2655–2664, https://doi.org/10.3892/mmr.2020.11378.

[14] J.Z. Hu, X.K. Wang, Y. Cao, D.Z. Li, T.D. Wu, T. Zhang, D.Q. Xu, H.B. Lu, Tetramethylpyrazine facilitates functional recovery after spinal cord injury by inhibiting MMP2, MMP9, and vascular endothelial cell apoptosis, Curr. Neurovascular Res. 14 (2017) 110–116, https://doi.org/10.2174/1567202614666170313114115.

[15] C. Wang, P. Wang, W. Zeng, W. Li, Tetramethylpyrazine improves the recovery of spinal cord injury via Akt/Nrf2/HO-1 pathway, Bioorg. Med. Chem. Lett 26 (2016) 1287–1291, https://doi.org/10.1016/j.bmcl.2016.01.015.

[16] Z. Shi, H. Zhou, L. Lu, X. Li, Z. Fu, J. Liu, Y. Kang, Z. Wei, B. Pan, L. Liu, et al., The roles of microRNAs in spinal cord injury, Int. J. Neurosci. 127 (2017) 1104–1115, https://doi.org/10.1080/00207454.2017.1323208.

[17] K. He, W.X. Li, D. Guan, M. Gong, S. Ye, Z. Fang, J.F. Huang, A. Lu, Regulatory network reconstruction of five essential microRNAs for survival analysis in breast cancer by integrating miRNA and mRNA expression datasets, Funct. Integr. Genom. 19 (2019) 645–658, https://doi.org/10.1007/s10142-019-00670-7.

[18] H.L. Chang, H.C. Wang, Y.T. Chunag, C.W. Chou, I.L. Lin, C.S. Lai, L.L. Chang, K.I. Cheng, miRNA expression change in dorsal root ganglia after peripheral nerve injury, J. Mol. Neurosci. : M. Inc. 61 (2017) 169–177, https://doi.org/10.1007/s12031-016-0876-7.

[19] F. Zhou, X. Jia, Y. Yang, Q. Yang, C. Gao, S. Hu, Y. Zhao, Y. Fan, X. Yuan, Nanofiber-mediated microRNA-126 delivery to vascular endothelial cells for blood vessel regeneration, Acta Biomater. 43 (2016) 303–313, https://doi.org/10.1016/j.actbio.2016.07.048.

[20] J.R. Finnerty, W.X. Wang, S.S. Hébert, B.R. Wilfred, G. Mao, P.T. Nelson, The miR-15/107 group of microRNA genes: evolutionary biology, cellular functions, and roles in human diseases, J. Mol. Biol. 402 (2010) 491–509, https://doi.org/10.1016/j.jmb.2010.07.051.

[21] X. Chen, C. Shi, C. Wang, W. Liu, Y. Chu, Z. Xiang, K. Hu, P. Dong, X. Han, The role of miR-497-5p in myofibroblast differentiation of LR-MSCs and pulmonary fibrogenesis, Sci. Rep. 7 (2017), 40958, https://doi.org/10.1038/srep40958.

[22] A. Mizrahi, A. Barzilai, D. Gur-Wahnon, I.Z. Ben-Dov, S. Glassberg, T. Meningher, E. Elharar, M. Masalha, J. Jacob-Hirsch, H. Tabibian-Keissar, et al., Alterations of microRNAs throughout the malignant evolution of cutaneous squamous cell carcinoma: the role of miR-497 in epithelial to mesenchymal transition of keratinocytes, Oncogene 37 (2018) 218–230, https://doi.org/10.1038/onc.2017.315.

[23] L. Chai, X.J. Kang, Z.Z. Sun, M.F. Zeng, S.R. Yu, Y. Ding, J.Q. Liang, T.T. Li, J. Zhao, MiR-497-5p, miR-195-5p and miR-455-3p function as tumor suppressors by targeting hTERT in melanoma A375 cells, Cancer Manag. Res. 10 (2018) 989–1003, https://doi.org/10.2147/cmar.S163335.

[24] L. Feng, K. Cheng, R. Zang, Q. Wang, J. Wang, miR-497-5p inhibits gastric cancer cell proliferation and growth through targeting PDK3, Biosci. Rep. 39 (2019), https://doi.org/10.1042/bsr20190654.

[25] Z. He, LINC00473/miR-497-5p regulates esophageal squamous cell carcinoma progression through targeting PRKAA1, Cancer Biother. Rad. 34 (2019) 650–659, https://doi.org/10.1089/cbr.2019.2875.

[26] H. Chang, J. Li, K. Qu, Y. Wan, S. Liu, W. Zheng, Z. Zhang, C. Liu, CRIF1 overexpression facilitates tumor growth and metastasis through inducing ROS/NFκB pathway in hepatocellular carcinoma, Cell Death Dis. 11 (2020) 332, https://doi.org/10.1038/s41419-020-2528-7.

[27] W. Zhu, H. Zhang, J. Gao, Y. Xu, Silencing of miR-497-5p inhibits cell apoptosis and promotes autophagy in Parkinson's disease by upregulation of FGF2, Environ. Toxicol. 36 (2021) 2302–2312, https://doi.org/10.1002/tox.23344.

[28] S.H. Su, C.H. Wu, Y.L. Chiu, S.J. Chang, H.H. Lo, K.H. Liao, C.F. Tsai, T.N. Tsai, C.H. Lin, S.M. Cheng, et al., Dysregulation of vascular endothelial growth factor receptor-2 by multiple miRNAs in endothelial colony-forming cells of coronary artery disease, J. Vasc. Res. 54 (2017) 22–32, https://doi.org/10.1159/000449202.

[29] G. Hong, V. Kuek, J. Shi, L. Zhou, X. Han, W. He, J. Tickner, H. Qiu, Q. Wei, J. Xu, EGFL7: Master regulator of cancer pathogenesis, angiogenesis and an emerging mediator of bone homeostasis, J. Cell. Physiol. 233 (2018) 8526–8537, https://doi.org/10.1002/jcp.26792.

[30] Q. Li, K. Cheng, A.Y. Wang, Q.G. Xu, Z.F. Fu, S.Y. He, P.X. Xu, microRNA-126 inhibits tube formation of HUVECs by interacting with EGFL7 and down-regulating PI3K/AKT signaling pathway, Biomedicine & pharmacotherapy = Biomedecine & pharmacotherapie 116 (2019), 109007, https://doi.org/10.1016/j.biopha.2019.109007.

[31] R. Usuba, J. Pauty, F. Soncin, Y.T. Matsunaga, EGFL7 regulates sprouting angiogenesis and endothelial integrity in a human blood vessel model, Biomaterials 197 (2019) 305–316, https://doi.org/10.1016/j.biomaterials.2019.01.022.

[32] J.K. Alexander, P.G. Popovich, Neuroinflammation in spinal cord injury: therapeutic targets for neuroprotection and regeneration, Prog. Brain Res. 175 (2009) 125–137, https://doi.org/10.1016/s0079-6123(09)17508-8.

[33] D.M. Basso, M.S. Beattie, J.C. Bresnahan, A sensitive and reliable locomotor rating scale for open field testing in rats, J. Neurotrauma 12 (1995) 1–21, https://doi.org/10.1089/neu.1995.12.1.

[34] R.J. Carter, J. Morton, S.B. Dunnett, Motor coordination and balance in rodents, Current protocols in neuroscience (2001), https://doi.org/10.1002/0471142301.ns0812s15 (Chapter 8), Unit 8.12.

[35] G. Bai, L. Jiang, P. Meng, J. Li, C. Han, Y. Wang, Q. Wang, LncRNA Neat1 promotes regeneration after spinal cord injury by targeting miR-29b, J. Mol. Neurosci. : M. Inc. 71 (2021) 1174–1184, https://doi.org/10.1007/s12031-020-01740-3.

[36] P. Hang, C. Sun, J. Guo, J. Zhao, Z. Du, BDNF-Mediates down-regulation of MicroRNA-195 inhibits ischemic cardiac apoptosis in rats, Int. J. Biol. Sci. 12 (2016) 979–989, https://doi.org/10.7150/ijbs.15071.
[37] X. Chen, Q. Zhang, Q. Cheng, F. Ding, Protective effect of salidroside against H2O2-induced cell apoptosis in primary culture of rat hippocampal neurons, Mol. Cell. Biochem. 332 (2009) 85–93, https://doi.org/10.1007/s11010-009-0177-3.
[38] Z. Shao, L. Wang, S. Liu, X. Wang, Tetramethylpyrazine protects neurons from oxygen-glucose deprivation-induced death, Med. Sci. Mon. Int. Med. J. Exp. Clin. Res. : international medical journal of experimental and clinical research 23 (2017) 5277–5282, https://doi.org/10.12659/msm.904554.
[39] N. Cui, H. Lu, M. Li, Q. Yan, PTPN21 protects PC12 cell against oxygen-glucose deprivation by activating cdk5 through ERK1/2 signaling pathway, Eur. J. Pharmacol. 814 (2017) 226–231, https://doi.org/10.1016/j.ejphar.2017.08.021.
[40] L. Lin, H. Liang, Y. Wang, X. Yin, Y. Hu, J. Huang, T. Ren, H. Xu, L. Zheng, X. Chen, microRNA-141 inhibits cell proliferation and invasion and promotes apoptosis by targeting hepatocyte nuclear factor-3β in hepatocellular carcinoma cells, BMC Cancer 14 (2014) 879, https://doi.org/10.1186/1471-2407-14-879.
[41] Y. Hu, Q. Liu, M. Zhang, Y. Yan, H. Yu, L. Ge, MicroRNA-362-3p attenuates motor deficit following spinal cord injury via targeting paired box gene 2, J. Integr. Neurosci. 18 (2019) 57–64, https://doi.org/10.31083/j.jin.2019.01.12.
[42] M. Guo, Y. Liu, D. Shi, Cardiovascular actions and therapeutic potential of tetramethylpyrazine (active component isolated from rhizoma chuanxiong): roles and mechanisms, BioMed Res. Int. 2016 (2016), 2430329, https://doi.org/10.1155/2016/2430329.
[43] L. Zhang, X. Wang, X. Lu, Y. Ma, X. Xin, X. Xu, S. Wang, Y. Hou, Tetramethylpyrazine enhanced the therapeutic effects of human umbilical cord mesenchymal stem cells in experimental autoimmune encephalomyelitis mice through Nrf2/HO-1 signaling pathway, Stem Cell Res. Ther. 11 (2020) 186, https://doi.org/10.1186/s13287-020-01700-z.
[44] J. Hu, Y. Cao, T. Wu, D. Li, H. Lu, Micro-CT as a tool to investigate the efficacy of tetramethylpyrazine in a rat spinal cord injury model, Spine 41 (2016) 1272–1278, https://doi.org/10.1097/brs.0000000000001546.
[45] J.H. Huang, Y. Cao, L. Zeng, G. Wang, M. Cao, H.B. Lu, J.Z. Hu, Tetramethylpyrazine enhances functional recovery after contusion spinal cord injury by modulation of MicroRNA-21, FasL, PDCD4 and PTEN expression, Brain Res. 1648 (2016) 35–45, https://doi.org/10.1016/j.brainres.2016.07.023.
[46] J. Hu, Y. Lang, Y. Cao, T. Zhang, H. Lu, The neuroprotective effect of tetramethylpyrazine against contusive spinal cord injury by activating PGC-1α in rats, Neurochem. Res. 40 (2015) 1393–1401, https://doi.org/10.1007/s11064-015-1606-1.
[47] X.Y. Bai, X.F. Wang, L.S. Zhang, P.C. Du, Z. Cao, Y. Hou, Tetramethylpyrazine ameliorates experimental autoimmune encephalomyelitis by modulating the inflammatory response, Biochem. Biophys. Res. Commun. 503 (2018) 1968–1972, https://doi.org/10.1016/j.bbrc.2018.07.143.
[48] Y. Fan, Y. Wu, Tetramethylpyrazine alleviates neural apoptosis in injured spinal cord via the downregulation of miR-214-3p, Biomedicine & pharmacotherapy = Biomedecine & pharmacotherapie 94 (2017) 827–833, https://doi.org/10.1016/j.biopha.2017.07.162.
[49] S. Zheng, J. Hou, Y. Chang, D. Zhao, H. Yang, J. Yang, CircRNA circ-CCND1 aggravates hepatocellular carcinoma tumorigenesis by regulating the miR-497-5p/HMGA2 Axis, Mol. Biotechnol. 64 (2022) 178–186, https://doi.org/10.1007/s12033-021-00391-y.
[50] D. Zhang, X. Chen, D. Zheng, A novel mir503hg/miR-497-5p/CCL19 Axis regulates high glucose-induced cell apoptosis, inflammation, and fibrosis in human HK-2 cells, Appl. Biochem. Biotechnol. 194 (2022) 2061–2076, https://doi.org/10.1007/s12010-021-03776-6.
[51] G. Villain, E. Lelievre, T. Broekelmann, O. Gayet, C. Havet, E. Werkmeister, R. Mecham, N. Dusetti, F. Soncin, V. Mattot, MAGP-1 and fibronectin control EGFL7 functions by driving its deposition into distinct endothelial extracellular matrix locations, FEBS J. 285 (2018) 4394–4412, https://doi.org/10.1111/febs.14680.